THE JOURNAL OF BIOLOGICAL CHEMISTRY VOL. 285, NO. 20, pp. 15557–15565, May 14, 2010

Escherichia coli α-Hemolysin Triggers Shrinkage of Erythrocytes via $K_{Ca}3.1$ and TMEM16A Channels with Subsequent Phosphatidylserine Exposure*[S]

Received for publication, November 5, 2009, and in revised form, February 21, 2010 Published, JBC Papers in Press, March 15, 2010, DOI 10.1074/jbc.M109.082578

Marianne Skals[‡], Uffe B. Jensen[§], Jiraporn Ousingsawat[¶], Karl Kunzelmann[¶], Jens Leipziger[‡], and Helle A. Praetorius[‡1]

From the [‡]Department of Physiology and Biophysics, Aarhus University, 8000 Aarhus, Denmark, the [§]Institute of Human Genetics, Aarhus University, and Department of Clinical Genetics, Aarhus University Hospital, 8000 Aarhus, Denmark, and the [¶]Department of Physiology, University of Regensburg, 93053 Regensburg, Germany

α-Hemolysin from *Escherichia coli* (HlyA) readily lyse erythrocytes from various species. We have recently demonstrated that this pore-forming toxin provokes distinct shrinkage and crenation before it finally leads to swelling and lysis of erythrocytes. The present study documents the underlying mechanism for this severe volume reduction. We show that HlyA-induced shrinkage and crenation of human erythrocytes occur subsequent to a significant rise in $[Ca^{2+}]_i$. The Ca^{2+}-activated K^+ channel $K_{Ca}3.1$ (or Gardos channel) is essential for the initial shrinkage, because both clotrimazole and TRAM-34 prevent the shrinkage and potentiate hemolysis produced by HlyA. Notably, the recently described Ca^{2+}-activated Cl^- channel TMEM16A contributes substantially to HlyA-induced cell volume reduction. Erythrocytes isolated from TMEM16A$^{-/-}$ mice showed significantly attenuated crenation and increased lysis compared with controls. Additionally, we found that HlyA leads to acute exposure of phosphatidylserine in the outer leaflet of the plasma membrane. This exposure was considerably reduced by $K_{Ca}3.1$ antagonists. In conclusion, this study shows that HlyA triggers acute erythrocyte shrinkage, which depends on Ca^{2+}-activated efflux of K^+ via $K_{Ca}3.1$ and Cl^- via TMEM16A, with subsequent phosphatidylserine exposure. This mechanism might potentially allow HlyA-damaged erythrocytes to be removed from the bloodstream by macrophages and thereby reduce the risk of intravascular hemolysis.

α-Hemolysin (HlyA)[2] produced by *Escherichia coli* is one of the key virulence factors released by invading *E. coli* strains. HlyA inserts into the plasma membrane and makes the cells permeable to cations and water (1–3). In erythrocytes, this increase in ion permeability has been established to result in swelling and ultimately lysis. We have recently discovered that the full hemolytic process requires purinergic signaling, because extracellular ATP scavenging and P2 receptor blockage completely abolished HlyA-induced hemolysis. Additionally, the HlyA-induced swelling and lysis is preceded by a substantial volume reduction in human and murine erythrocytes (4). This sequential shrinkage and swelling was observed in single cells as an initial crenation, followed by swelling/spherocyte formation before the final lysis (4).

The initial volume decrease induced by HlyA is surprising because it implies that insertion of the pore results in a net ion efflux rather than an influx. Because K^+ quantitatively is the most important intracellular cation, this effectively means that the K^+ efflux during the shrinkage is larger than the Na^+ influx. This notion is supported by the large K^+ efflux, which can be observed within 1–2 min after HlyA addition (2, 5). Because HlyA is a nonselective pore, permeable to both mono- and divalent cations (6), it is unlikely to show a preference for K^+ over Na^+. Human erythrocytes have a resting membrane potential of approximately −5 to −10 mV (7), which is close to the reversal potential of any nonselective cation channel. Thus, it is very hard to imagine that insertion of a nonselective pore *per se* would result in a selective K^+ conductance. This would require either a selectivity of the pore and/or a favorable driving force for K^+ over Na^+. Therefore, we speculated that insertion of HlyA pores activates K^+ and possibly Cl^- selective ion channels natively present in the erythrocytes. This activation could be responsible for the observed HlyA-induced volume reduction, a process that potentially will protect the erythrocytes against immediate lysis.

We here investigate the underlying mechanism for the marked HlyA-induced volume reduction of red blood cells. We were able to show that HlyA-induced shrinkage is a consequence of a rise in the intracellular Ca^{2+} concentration ($[Ca^{2+}]_i$), which triggers activation of K^+ channels (KCa3.1/Gardos channel) and Cl^- channels (TMEM16A), with a subsequent exposure of phosphatidylserine (PS) in the outer leaflet of the membrane. Because macrophages recognize and phagocytose PS exposing erythrocytes, the early volume regulations may be important for removal of HlyA-damaged erythrocytes from the bloodstream.

MATERIALS AND METHODS

Preparations of Human and Murine Erythrocytes—Blood samples from eight healthy volunteers were collected in EDTA-containing tubes and washed twice (1000 × *g*, 1 min at 4 °C) in

* This work was supported by the Danish Medical Research Council, the Danish National Research Foundation, and German Research Foundation Grants SFB699 A6/A7 and KU 756/8-2. The Water and Salt Research Center at the Aarhus University is established and supported by the Danish National Research Foundation (Danmarks Grundforskningsfond).

[S] The on-line version of this article (available at http://www.jbc.org) contains supplemental Figs. S1–S4.

[1] To whom correspondence should be addressed: Dept. of Physiology and Biophysics, Aarhus University, Ole Worms Allé 1180, 8000 Aarhus C, Denmark. E-mail: hp@fi.au.dk.

[2] The abbreviations used are: HlyA, α-hemolysin; PS, phosphatidylserine; DIC, differential interference contrast; FSC, forward scatter; SSC, side scatter.

0.9% NaCl, the buffy coat was removed, and the remaining cells were washed twice in Ca^{2+}-containing saline. The experiments were approved by the Danish National Committee on Biomedical Research Ethics. TMEM16A-deficient ($TMEM16A^{-/-}$) and littermate control ($TMEM16A^{+/+}$) mice (8) on C57BL6 background were bred at the University of Regensburg, where the experiments with erythrocytes from TMEM16A mice were performed according to the national guidelines for care and use of animals in research and the German law on protection of animals. The animals were killed 1–3 days after birth by cervical dislocation, and the blood was collected in heparin-containing tubes and prepared similar to the human erythrocytes. Age-matched $CFTR^{+/+}$ and $CFTR^{-/-}$ mice were kindly supplied by Ursula Seidler (Hannover Medical School, Hannover, Germany) and used when 12–16 weeks old. $AQP1^{+/+}$ and littermate $AQP1^{-/-}$ mice were bred at the Department of Anatomy of Aarhus University and originally supplied by Alan Verkman (University of California). The APQ1 mice were used when they were 14 weeks old.

α-Hemolysin—The majority of the experiments were performed with purified α-hemolysin from *E. coli* kindly provided by Sucharit Bhakdi (University of Mainz, Mainz, Germany). For the $CFTR^{+/+}$ *versus* $CFTR^{-/-}$ and $AQP1^{+/+}$ *versus* $AQP1^{-/-}$ erythrocytes (supplemental Fig. S2), as well as the experiments with niflumic acid on murine erythrocytes (supplemental Fig. S3), native HlyA in the supernatant from the *E. coli* strain ARD6 (Statens Serum Institut, Copenhagen, Denmark) was used. The bacterial strain ARD6 secretes HlyA (for further details see Ref. 4). The purified HlyA was supplied at a stock concentration of 50 μg ml^{-1}, and the concentration was adjusted to result in either 0, 20, 50, or 100% hemolysis depending on the various experiments in a preparation of either 1.25% (measurements of released hemoglobin) or 0.02% erythrocytes (flow cytometry). For further specifics see legends to figures.

Imaging of Shrinkage and Hemolysis of $TMEM16A^{+/+}$ and $TMEM16A^{-/-}$ Murine Erythrocytes—The red blood cells were attached to coverslips by Cell-Tak™ (BD Biosciences) and placed on an inverted microscope (Axiovert 200M; Zeiss) at room temperature. Time lapse recordings of the erythrocyte appearance in differential interference contrast (DIC) (63×, NA1.2) were collected over 60 min after the addition of HlyA (sampling rate was 1 picture every 10 s for the first 5 min and thereafter every 30 s using the program AxioVision from Zeiss). The change in erythrocyte shape and lysis was compared between the two genotypes.

Measurements of Hemolytic Activity—The erythrocytes were suspended (1.25%) in Ca^{2+}-containing saline. The hemolytic activity was measured spectrophotometrically (Ultraspec III, LKB Biochrom, Cambridge, UK) at 540 nm. HlyA was added (5 or 10 ng ml^{-1}, resulting in 20 or 50% lysis) in 1.5-ml test tubes with or without antagonists (clotrimazole or TRAM-34) and placed in an incubation chamber (ES-20; Biosan, Riga, Latvia) for 60 min at 37 °C under a constant swirl of 200 rpm. Thereafter, the tubes were centrifuged (1000 × *g*, 3 min, 4 °C), and the A_{540} of the supernatant was determined as a measure of released hemoglobin.

Flow Cytometry—Flow cytometry analysis was performed on a FACSAria flow cytometer (BD Biosciences), using BD FACSDiVa software for acquisition and analysis. Erythrocyte size and density were assessed using forward scatter (FSC) and side scatter (SSC), respectively. All of the experiments were performed using a 100-μm nozzle and a standard sheet pressure of 20 p.s.i. For all of the experiments, a suspension of isolated erythrocytes (0.02%) containing ~10^6 cells ml^{-1} was used. For the time course experiments, the effect of HlyA was investigated from 0 to 45 min in the presence or absence of clotrimazole or TRAM-34. The flow rate was adjusted to keep the cell count at 1000 events s^{-1}.

Annexin V Binding—For the annexin V binding studies, 10^5 cells were investigated per experimental condition. The erythrocytes were incubated with HlyA (1 ng ml^{-1}, resulting in 15–20% shrinkage but 0% lysis) for 10 min at room temperature. Afterward they were centrifuged for 3 min at 1000 × *g*, before they were resuspended in a solution composed of annexin V and annexin V binding buffer (dilution, 1:50; Roche Diagnostics GmbH, Mannheim, Germany) and incubated in the dark for 10 min. The suspension was diluted 1/5 in a Ca^{2+}-containing saline, and the sample was run on the flow cytometer. All of the experiments were conducted at 37 °C, 488-nm excitation/520-nm emission. $[Ca^{2+}]_i$ measurements were also performed on the FACSaria flow cytometer. Isolated erythrocytes (~10^6 cells ml^{-1}) were preincubated for 25 min in fluo 4-AM (5 μM) (Invitrogen) at 37 °C and washed once in Ca^{2+}-containing saline (1000 × *g* for 3 min at room temperature). The time-dependent increase in 488-nm fluorescence was measured after HlyA addition (3 ng ml^{-1}) in parallel with FSC and SSC.

$[Ca^{2+}]_i$ Imaging of Human Erythrocytes—Human erythrocytes attached to coverslips by Cell-Tak™ (BD Bioscience) were incubated with fluo 4 (5 μM) for 25 min at 37 °C, washed once, and placed on the stage of an inverted microscope (TE-2000; Nikon). Low level excitation light was provided by a monochromator (Visitech International, Sunderland, UK). Time lapse recordings of the erythrocyte appearance in DIC (63×, NA1.2) were collected over 15 min after the addition of HlyA (sampling rate, 0.1 Hz) using an intensified SVGA charge-coupled device camera and imaging software (Quanticell 2000/Image Pro; Visi-Tech). Fluo 4 was excited at 488 nm, and emission was detected above 520 nm. All of the experiments were carried out at 37 °C and pH 7.4. In these experiments 0.1% bovine albumin serum was added to the medium to avoid crenation of the erythrocytes, which usually is seen as they come in contact with the coverslip glass surface (9).

Solutions and Materials—The Ca^{2+}-containing saline contained 138.0 mM [Na^+], 132.9 mM [Cl^-], 5.3 mM [K^+], 1.8 mM [Ca^{2+}], 0.8 mM [Mg^{2+}], 0.8 mM [SO_4^{2-}], 14.0 mM [Hepes], and 5.6 mM [glucose], pH 7.4 at 37 °C. Bovine albumin serum, clotrimazole, and TRAM-34 were obtained from Sigma. All of the reagents were dissolved in isotonic saline and pH adjusted to 7.4 at 37 °C. Clotrimazole and TRAM-34 were dissolved in Me_2SO to a final concentration of maximally 0.5% Me_2SO. Control experiments to test the effect of Me_2SO alone were conducted and showed no interference with the results.

Data Analysis and Statistics—The data are presented as the means± S.E. The *n* value indicates number of individuals or mice. The data were tested for normal distribution by Kolmogorov-

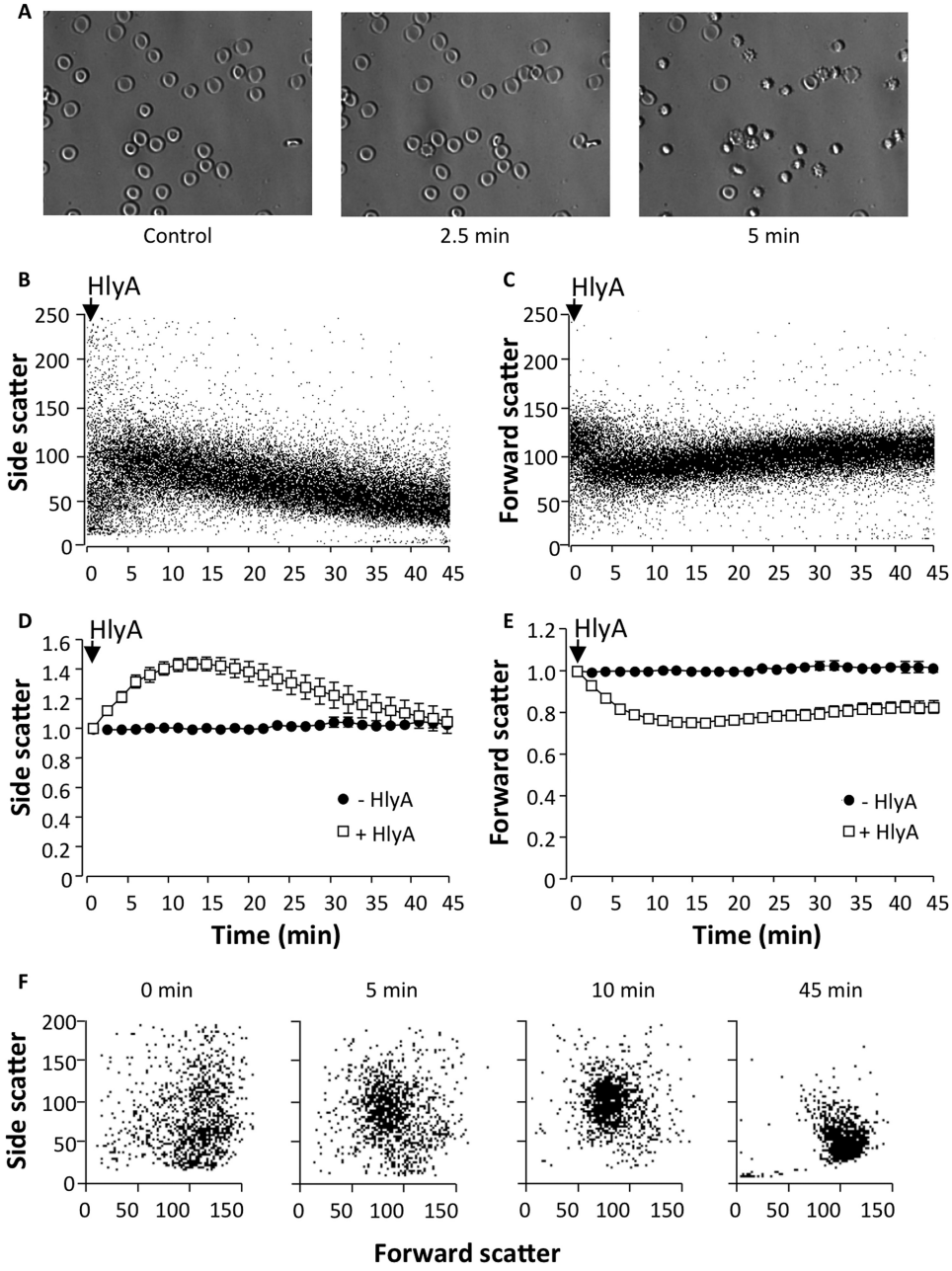

FIGURE 1. **Volume changes in human erythrocytes induced by HlyA from *E. coli*.** *A*, representative DIC images of erythrocytes before and after HlyA stimulation (~25 ng ml^{-1}). *B* and *C*, representative traces showing side scatter (*B*) and forward scatter (*C*) over time (0–45 min) after HlyA (3 ng ml^{-1}) is applied. Each dot represents a single erythrocyte. The values on the *y* axis are arbitrary. *D* and *E*, mean normalized values of side scatter (*D*) and forward scatter (*E*) over time (0–45 min) after HlyA (3 ng ml^{-1}) is applied (*open squares*) and time controls (*filled circles*). *F*, side scatter as a function of forward scatter at four time points (0, 5, 10, and 45 min) after HlyA is added (3 ng ml^{-1}). Each *dot* represents a single erythrocyte. The values on the axis are arbitrary and shown as the means ± S.E. ($n = 8$).

Smirnov test. Significant differences were determined by paired or unpaired Student's *t* test or one-way analysis of variance (Tukey post test) for multiple comparisons as appropriate. In both cases a *p* value less than 0.05 was considered statistically significant.

RESULTS

HlyA from E. coli Induces Shrinkage, Swelling, and Lysis of Human Erythrocytes—Previously we have reported that HlyA produces a significant shrinkage of erythrocytes before they finally swell and lyse. Here we use flow cytometry to verify the volume changes we previously observed in transmission microscopy with DIC. First, we confirmed our previous findings with DIC images. Fig. 1*A* shows images of human erythrocytes 0, 2.5, and 5 min after HlyA stimulation (25 ng ml^{-1}). Similar results were obtained with HlyA-containing *E. coli* supernatant (data not shown). Clear shrinkage and crenation of the cells were observed within 5 min of HlyA stimulation. The FSC is generally used directly as reflection of cell volume, whereas SSC reports the morphological complexity of the cell. The SSC can, however, also be used as a measure of cell volume changes. It was shown that cell volume reduction is proportional to an increased wide angle light scatter (10), which is equivalent to the SSC in the flow cytometer. The erythrocyte suspension showed a marked decrease in FSC and an increase in SSC within the first 10 min after the addition of HlyA (3 ng ml^{-1}). The decrease in FSC and the increase in SSC occur simultaneously with the crenation of the erythrocytes when viewed in the microscope (Fig. 1, *A* and *B*). Because of the close temporal association between changes in FSC and SSC and the morphological changes observed on the microscope, we consider the reduction of FSC and the increase in SSC as erythrocyte shrinkage and crenation. Over time, the initial SSC increase and FSC decrease slowly recovered, reflecting the subsequent cell swelling. Fig. 1 (*B* and *C*) shows representative experiments of human erythrocytes exposed to HlyA (3 ng ml^{-1}) over time, and mean values FSC and SSC are shown in Fig. 1 (*D* and *E*). A similar pattern was observed when the HlyA concentration was increased to (10 ng ml^{-1}), which resulted in 100% hemolysis in erythrocyte suspension of 0.02% (supplemental Fig. S1, *A*–*C*). Please note that the initial population of erythrocytes shows significant diversity in FSC, reflecting the biconcave shape of the erythrocytes and the random way they pass the laser beam in the flow cytometer. After HlyA is added, the population becomes more uniform because the biconcave shape is lost when the cells shrink and swell (Fig. 1*F*). Similar results were seen with HlyA-containing *E. coli* supernatant (data not shown).

HlyA Provokes an Increase in $[Ca^{2+}]_i$ in Human Erythrocytes—HlyA is known to insert into the erythrocyte membrane and creates pores that render the membrane permeable to smaller cations. The significant HlyA-induced shrinkage of the cells implies that the K^+ conductance of the erythrocyte was initially much larger than the overall cellular Na^+ conductance. HlyA insertion is likely to activate a selective K^+ conductance, which presumably is the Ca^{2+}-activated K^+ channel, $K_{Ca}3.1$, or Gardos. Therefore, we investigated whether HlyA triggers changes in $[Ca^{2+}]_i$. Fig. 2*A* shows a representative experiment indicating the change in fluo 4 fluorescence in a population of erythrocytes over time after the addition of HlyA (3 ng ml^{-1}). Within 2 min, there is a pronounced increase of the population of red blood cells showing $[Ca^{2+}]_i$ increase (cells marked by *red bars*). In Fig. 2*B* one can observe that the increase in $[Ca^{2+}]_i$ (marked in *red*), the cell volume reduction, and crenation (decrease in FSC and increase in SSC) coincide in a subpopulation of erythrocytes at times 0, 2, 6, and 10 min after the addition of HlyA. Fig. 2*C* shows the equivalent effect of ionomycin (1 μM) on $[Ca^{2+}]_i$ as a positive control. After 10 min all of the cells show an increase in $[Ca^{2+}]_i$(marked in *red*), with a simultaneous rise in SSC and a decrease in FSC (which equals cell shrinkage) induced by ionomycin. The percentage of cells that respond to HlyA with an increase in $[Ca^{2+}]_i$ ($[Ca^{2+}]_i$ increasing cells) increase with the time of incubation (Fig. 2*D*). Again, ionomycin (1 μM) is used as a positive control (Fig. 2*E*). Similarly, HlyA induced a rise of 2.03 ± 0.24 ($n = 7$, with blood from three donors) in fluo-4 fluorescence when single erythrocytes were observed over time on an inverted microscope (Fig. 2*F*). The representative images of fluo 4-loaded erythrocytes clearly show that the $[Ca^{2+}]_i$ increase induced by HlyA occurs prior to shrinkage and crenation (Fig. 2*G*). The crenation starts

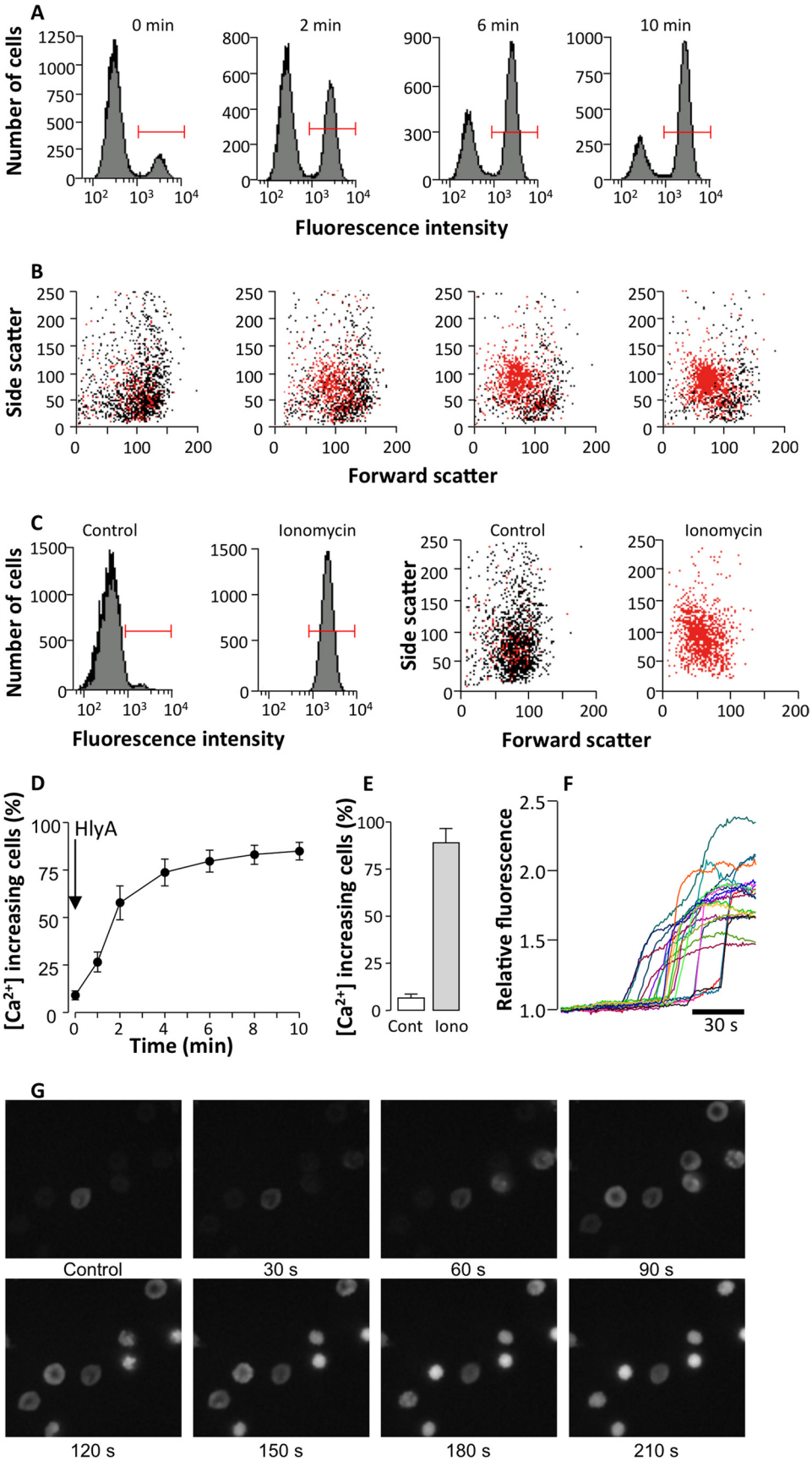

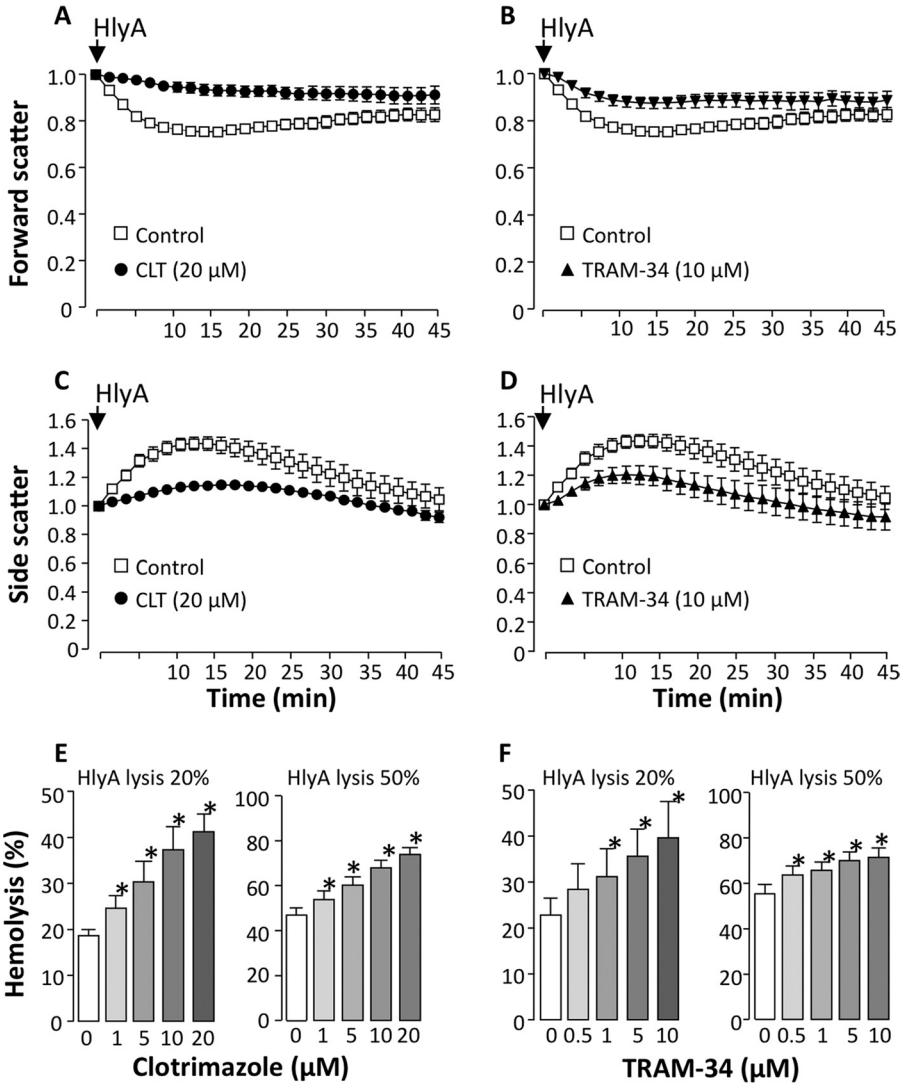

FIGURE 3. **The effect of K_{Ca}1. 3 channel inhibitors on HlyA-induced volume changes and lysis in human erythrocytes.** *A*, the effect of clotrimazole (*CLT*, 20 μM, *filled circles*) on the changes in forward scatter induced by HlyA (3 ng ml^{-1}) compared with controls (*open squares*). *B*, shows the effect of TRAM-34 (10 μM, *filled triangles*) on the change in forward scatter induced by HlyA (3 ng ml^{-1}) compared with controls (*open squares*). *C* and *D*, the corresponding changes in side scatter in response to clotrimazole and TRAM-34 are shown in *C* and *D*, respectively. All of the above values are normalized to time 0 and given as mean values ± S.E. (n = 5–6). The hemolysis was measured as the level of released hemoglobin in the absence or presence of increasing concentrations of clotrimazole (*E*) and TRAM-34 (*F*) at two concentrations of HlyA leading to 20 and 50% lysis after 60 min (5 and 10 ng ml^{-1}, respectively). The values are given as the means ± S.E. (n = 4–6).

73.2 ± 4.14 s after the increase in $[Ca^{2+}]_i$ (measured in 106 cells from six experiments, three donors).

HlyA Triggers an Activation of K_{Ca}3.1/Gardos Channel—Because our initial notion was that the shrinkage is the result of Ca^{2+}-activated K^+ efflux, we used two K_{Ca}3.1 channels antagonists, clotrimazole and TRAM-34, to address this question. At a concentration of 20 μM clotrimazole completely inhibited the initial changes in SSC and FSC after HlyA application (3 ng ml^{-1}) (Fig. 3, *A* and *B*). Very similar results were obtained with 10 μM TRAM-34 (Fig. 3, *C* and *D*). Lower concentrations of clotrimazole (5 μM) and TRAM-34 (1 μM) showed a partial but statistically significant inhibition of the forward scatter (supplemental Fig. S1*E*). TRAM-34 also had a considerable effect on the HlyA-induced shrinkage, *i.e.* a decrease in FSC and an increase in SSC, at a concentration of HlyA leading to 100% lysis (supplemental Fig. S1, *C* and *D*).

Because both K_{Ca}3.1 channel inhibitors significantly affect volume regulation in erythrocytes one would also expect them to influence the HlyA-induced hemolysis. Both clotrimazole and TRAM-34 potentiated the hemolytic effect of HlyA (Fig. 3, *E* and *F*). At concentrations that result in maximal inhibition of the HlyA-induced volume changes, both clotrimazol (20 μM) and TRAM-34 (10 μM) result in a doubling of hemolysis. In these experiments, the concentration of HlyA (5 ng ml^{-1}) was adjusted to produce 20% hemolysis after 60 min of incubation. At a concentration that causes 50% lysis (10 ng ml^{-1}), both antagonists led to ~1.4 times increase in hemolysis. These data strongly suggest that K_{Ca}3.1 channels are essential for the volume regulations provoked by HlyA, and activation of these channels makes the cells less susceptible to pore-forming toxins.

HlyA Activates the Ca^{2+}-dependent Cl^- Channel TMEM16A—Erythrocytes have a significant steady state Cl^- conductance (11, 12). Therefore, in principle, it should not be necessary to activate yet another Cl^- exit pathway to sustain the K^+ efflux during red cells shrinkage. Many cells do, however, show Ca^{2+}-

FIGURE 2. **Effect of HlyA on $[Ca^{2+}]_i$ in human erythrocytes.** *A*, number of cells as a function of fluo 4 fluorescence signal shows two populations of cells at time 0, 2, 6, and 10 min after HlyA is applied (3 ng ml^{-1}). The population of cells with a substantial rise in $[Ca^{2+}]_i$ (as indicated by the *red bars*) is defined as $[Ca^{2+}]_i$ increasing cells. *B*, side scatter as a function of forward scatter at time 0, 2, 6, and 10 min after HlyA is applied (3 ng ml^{-1}). The cells marked in *red* (the same population as marked with the *red bar* in *A* show a rise in $[Ca^{2+}]_i$. Each *dot* represents a single erythrocyte. The values on the axis are arbitrary. *C*, the corresponding effect of the Ca^{2+} ionophore, ionomycin. At the *left* the numbers of cells are shown as a function of fluo 4 fluorescence signal. Again during control there are two populations of cells, one with low and a smaller with higher $[Ca^{2+}]_i$. Only a single population of cells with high $[Ca^{2+}]_i$ was observed after ionomycin was applied (1 μM, 10 min). At the *right* the side scatter is shown as a function of forward scatter during control, and 10 min after ionomycin was applied. The cells marked in *red* (the same population as marked with a *red bar* in the *left panels*) show a rise in $[Ca^{2+}]_i$. Each *dot* represents a single erythrocyte. The values on the axis are arbitrary. *D*, the percentage of erythrocytes with a rise in $[Ca^{2+}]_i$ in response to HlyA. The values are the means ± S.E. (n = 5). *E*, the mean values of cells with a rise in $[Ca^{2+}]_i$ after addition of ionomycin (1 μM). The values are the means ± S.E. (n = 5). *F*, the traces show the change in fluo 4 fluorescence over time in 23 erythrocytes in response to HlyA. *G*, imaging of fluo 4-loaded human erythrocytes exposed to HlyA (25 ng ml^{-1}).

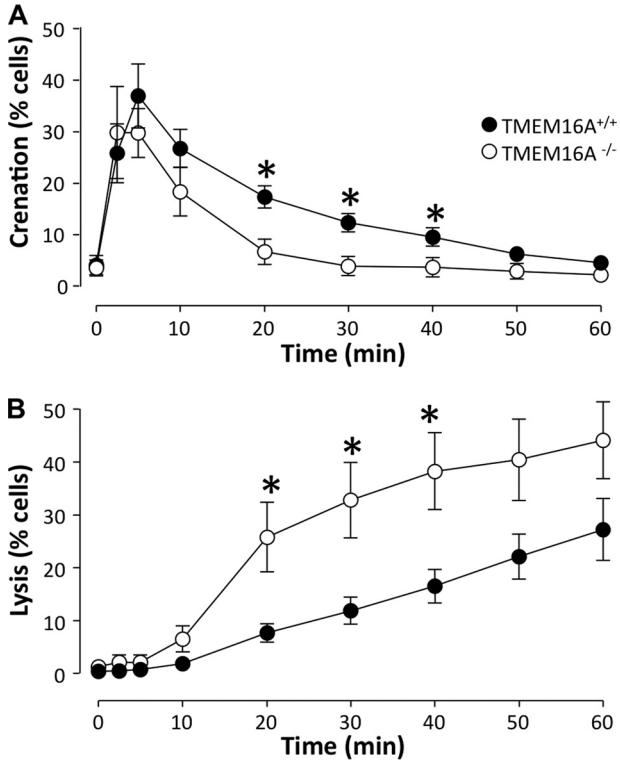

FIGURE 4. **HlyA-induced crenation and lysis in erythrocytes from TMEM16A$^{-/-}$ *versus* TMEM16A$^{+/+}$ mice.** *A*, the number of erythrocytes isolated from TMEM16A$^{+/+}$ and TMEM16A$^{-/-}$ mice, which crenate in response to HlyA (25 ng ml^{-1}). *B*, the subsequent lysis of erythrocytes isolated from TMEM16A$^{+/+}$ and TMEM16A$^{-/-}$ mice in response to HlyA. The values are given as the means ± S.E. (n = 8 for TMEM16A$^{+/+}$ mice and n = 6 for TMEM16A$^{-/-}$ mice). The *asterisks* indicate statistically significance between the values obtained from TMEM16A$^{-/-}$ and TMEM16A$^{+/+}$ mice.

activated Cl^- conductance. Here we tested whether the newly described Ca^{2+}-activated Cl^- channel TMEM16A is present in erythrocytes and activated by the HlyA-induced $[Ca^{2+}]_i$ increase. Because chloride channel blockers are generally nonselective, we chose to study the HlyA-induced hemolysis in TMEM16A-deficient mice (TMEM16A$^{-/-}$).

TMEM16A$^{-/-}$ mice have a severe phenotype, and the pups die within the first 2 weeks after birth (8, 13). We studied the erythrocytes using DIC microscopy and found a statistically significant difference between the HlyA-induced hemolysis in TMEM16A$^{-/-}$ and TMEM16A$^{+/+}$ mice. The TMEM16A$^{-/-}$ showed a considerably less shrinkage and a higher level of lysis relative to TMEM16A$^{+/+}$ mice, when incubated with HlyA (25 ng ml^{-1}; Fig. 4). These data are supported by the nonselective Cl^- channel blocker niflumic acid, which also potentiates the HlyA-induced hemolysis in murine erythrocytes (supplemental Fig. S3). Please note that murine erythrocytes are more sensitive to HlyA compared with human (4). The TMEM16A$^{+/+}$ and TMEM16A$^{-/-}$ mice had similar erythrocyte size, measured as the diameter of the cells when plated on coverslips. The diameter was 5.28 ± 0.04 μm in the TMEM16A$^{+/+}$ and 5.36 ± 0.05 in the TMEM16$^{-/-}$ erythrocytes (counted in 100 cells from five mice of each genotype), a similar hematocrit and reticulocyte count (supplemental Fig. S4). Furthermore, the osmotic resistance and the Coomassie SDS-PAGE were similar in the erythrocytes from TMEM16A$^{+/+}$ and TMEM16A$^{-/-}$ mice (supplemental Fig. S4).

Role of CFTR and Aquaporin 1—We also investigated the possible contribution of CFTR and aquaporin 1 in the HlyA-induced hemolysis. There was no detectable difference in the HlyA-induced hemolysis in CFTR$^{-/-}$ and AQP1$^{-/-}$ mice compared with wild type controls. In these experiments, we studied the level of released hemoglobin 60 min after HlyA (*E. coli* ARD6 supernatant, 25–50 μl ml^{-1}) application (supplemental Fig. S2).

HlyA Triggers PS Exposure in the Outer Leaflet—It is known that increments in erythrocyte Ca^{2+} concentration trigger an early senescent response in red blood cells with exposure of PS in the outer leaflet of the erythrocyte membrane (14). Therefore, we explored whether HlyA likewise would cause PS exposure. We used fluorescein isothiocyanate-conjugated annexin V, a substance with high affinity for PS.

To be able to quantify the PS content in the outer leaflet of the plasma membrane, one has to assure that the erythrocytes remain intact. Normally, dyes that bind to DNA as propidium iodide are used as indicators of cells with lost plasma membrane integrity. In mammalian erythrocytes, which are anucleated, this is not a very good marker of membrane integrity because the dye does not accumulate in the cells. Therefore, we used a very low concentration of HlyA (1 ng ml^{-1}) that only led to shrinkage of ~15–20% of the cells within 10 min and do not induce detectable cell lysis during our experimental conditions (Fig. 5). We found a significant annexin V staining of ~10% of the cells (Fig. 5, *D–F*). By comparing the highlighted regions in Fig. 5 (*B* and *E*), we observed that the cells that experience the fall in FSC and the increase in SSC also are the ones that show increased annexin V binding. Furthermore, we were able to confirm that inhibition of cell shrinkage also prevents PS exposure (15), because both clotrimazole and TRAM-34 significantly inhibited HlyA-induced PS exposure at a concentration of 1 μM (Fig. 5*G*). These results support that the HlyA-induced annexin V binding is not caused by cell lysis. If this was the case the K_{Ca}3.1 channel blockers, which amplify hemolysis, would have increased and not reduced HlyA-induced annexin V binding.

DISCUSSION

E. coli HlyA is well known to lyse erythrocytes by creating ~2-nm pores in the plasma membrane that allow influx of cations and water (1–3). Recently, we showed that HlyA-induced lysis requires ATP release and P2 receptor activation (4), and thus, the effect of HlyA pore insertion is amplified through purinergic signaling. We also observed that HlyA-induced lysis is a sequential process of initial shrinkage and crenation of human and murine erythrocytes, followed by swelling and lysis. In the present study, we investigated and defined the mechanism of HlyA-induced erythrocyte shrinkage.

By DIC imaging, we confirmed our previous finding that HlyA initially induces pronounced crenation of human red blood cells (4). We were able to substantiate that these HlyA-induced erythrocyte shape changes corresponded to cellular volume reductions by flow cytometry. HlyA triggered a marked decrease in FSC, reflecting a reduction of cell size and a simultaneous rise in SSC. Side scatter normally reports about the number of refraction surfaces of the cell as it passes through the

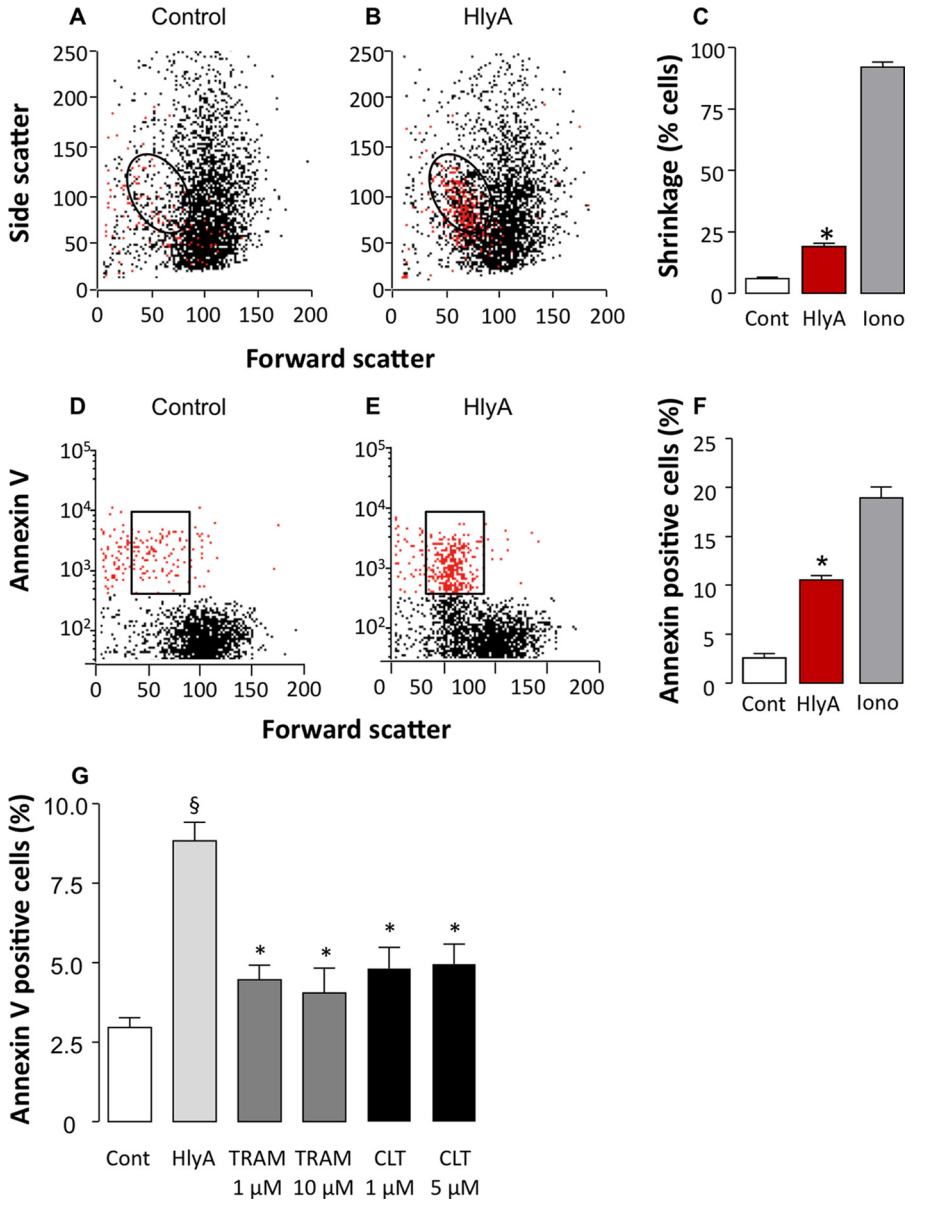

FIGURE 5. **HlyA induced PS exposure (annexin V binding) in human erythrocytes is inhibited by K_{Ca}1. 3 channel antagonists.** *A* and *B*, representative experiment showing side scatter as a function of forward scatter during control (*A*) and after HlyA (1 ng ml^{-1}) is applied (*B*). The HlyA concentration (1 ng ml^{-1}) was adjusted to completely avoid hemolysis during the observation period. The *circled regions* in *A* and *B* define shrunken cells. *C*, mean value of erythrocyte shrinkage after HlyA is applied ($n = 10$). Ionomycin (1 μM) was used as a positive control for cell shrinkage ($n = 5$). *D* and *E*, annexin V binding in the same cells as shown in A and B during control (*D*) and after HlyA is applied (*E*). The *boxed regions* define cells which are both shrunken and positive for annexin V staining. *F*, mean value of number of cells binding annexin V ($n = 10$). Ionomycin (1 μM) was used a positive control for annexin V binding ($n = 5$). *G*, K_{Ca}1.3 channel antagonists reduce HlyA-induced PS exposure in human erythrocytes. Erythrocytes incubated with annexin V during control and HlyA application (1 ng ml^{-1}) in the absence or presence of either TRAM-34 (1 and 10 μM) or clotrimazole (*CLT*, 1 and 5 μM). The values are given as the means ± S.E. ($n = 5$–7). The *asterisks* indicate statistical significance.

laser beam and thus conveys information about the morphological complexity of the given cell. It has been established that cell volume reduction is proportional to an increased wide angle light scatter (10), which is equivalent to the SSC in the flow cytometer. The combination of a reduction in FSC and a rise in SSC has previously been used to identify volume reduction in erythrocytes after exposure to Ca^{2+} ionophores (14, 16). The changes we observed in FSC and SSC occur simultaneously with cell shape changes observed on the microscope. Thus, we take these combined changes in SSC and FSC as an indication of erythrocyte shrinkage and crenation.

Because Ca^{2+} ionophores are known to trigger comparable changes in light scattering (14) and crenation (17, 18), we investigated whether HlyA caused a rise in $[Ca^{2+}]_i$. Flow cytometry of fluo 4-loaded human erythrocytes clearly showed that HlyA was able to produce an increase in $[Ca^{2+}]_i$, supporting earlier studies showing that HlyA produces an influx of Ca^{2+} (3, 6). Additionally, there was a clear correlation between erythrocytes with elevated $[Ca^{2+}]_i$ and reduced cell volume. By studying fluo 4-loaded single erythrocytes with $[Ca^{2+}]_i$ imaging, the $[Ca^{2+}]_i$ evidently rose prior to the cell shrinkage. To our knowledge, this is the first report of $[Ca^{2+}]_i$ changes preceding shrinkage of erythrocytes. In addition, the single cell $[Ca^{2+}]_i$ measurements indicate that HlyA-induced $[Ca^{2+}]_i$ increase is an all-or-none response. Either the cells showed a marked rise in $[Ca^{2+}]_i$, or the cells seemed completely unaffected by HlyA. Only on rare occasions were fluctuating $[Ca^{2+}]_i$ levels observed in single cells. Thus, it is tempting to speculate that only one or very few toxin molecules are necessary to trigger the cell damaging effects, supporting earlier studies (19, 20).

The precise Ca^{2+} entry mechanism for HlyA-induced $[Ca^{2+}]_i$ changes has not been settled. It is, however, very likely that Ca^{2+} enters the cell through HlyA itself because it has a significant Ca^{2+} conductance (5, 20). Ca^{2+} could also potentially enter through nonselective cation channels such as TRPC6 (21), P2X receptors (22), or via pannexin 1 channels (23), where the latter two are known to be activated upon HlyA exposure (4).

HlyA inflicts a substantial loss of K^+, which starts shortly after the erythrocytes have been subjected to the toxin (2, 5). Part of the total cellular K^+ loss results from lysis. However, the initial K^+ efflux, which occurs before there is substantial cell lysis, is likely to cause the extensive volume reduction seen in the early phases of HlyA-induced hemolysis. This resembles what has been observed with Ca^{2+} ionophores (17, 24). A good candidate for an activated K^+ efflux pathway is the K_{Ca}3.1

channel (SK_4 or Gardos channel); the only Ca^{2+}-activated K^+ channel known to be present in erythrocytes (25, 26). Activation of this channel causes erythrocyte dehydration, a mechanism crucial for sickle formation in sickle cell anemia (27). In line with this, we found that inhibitors of K_{Ca}3.1, clotrimazole, and TRAM-34 blocked the HlyA-induced shrinkage. This is consistent with reduced Ca^{2+} ionophore-induced erythrocyte shrinkage in K_{Ca}3.1-deficient mice (28), and it is reasonable to conclude that the HlyA-induced shrinkage is caused by Ca^{2+}-activated K^+ efflux through K_{Ca}3.1 channels. Preventing the cell volume reduction inflicted by K_{Ca}3.1 channels by either clotrimazole or TRAM-34 clearly potentiated the hemolysis induced by HlyA. This supports previous data showing that $K_{Ca}3.1^{-/-}$ mice are more susceptible to osmotically (28) and α-toxin-induced hemolysis (29). Thus, our data support that cell shrinkage is a protective mechanism to avoid acute lysis. Cellular K^+ efflux occurs concomitantly with anion efflux, and erythrocytes do have a significant resting Cl^- conductance (11, 12). Therefore, we speculated that a substantial increase in K^+ efflux might require activation of additional Cl^- channels, which could implicate the function of a Ca^{2+}-activated Cl^- channel in erythrocytes.

The poor selectivity of Cl^- channel antagonist makes it difficult to dissect eventual activation of an additional Cl^- conductive pathway during HlyA-induced erythrocyte shrinkage. Nonselective Cl^- channel blockers such as NPPB and niflumic acid have been shown to counteract the Ca^{2+} ionophore-induced cell shrinkage in human erythrocytes (30). Recently, the protein TMEM16A (or ANO1) has been substantiated as a Ca^{2+}-activated Cl^- channel and has been shown to play a role in volume regulation of colonic epithelial and salivary acinar cells (13). Therefore, we compared $TMEM16A^{-/-}$ *versus* $TMEM16A^{+/+}$ murine erythrocytes from newborn littermates. Erythrocytes from $TMEM16A^{-/-}$ mice showed a significantly lower level of HlyA-induced shrinkage compared with $TMEM16A^{+/+}$. As a consequence, lysis of $TMEM16A^{-/-}$ erythrocytes occurs much faster than $TMEM16A^{+/+}$ controls. The $TMEM16A^{-/-}$ cells were still able to shrink and thus, not surprisingly other anion channels contribute overall volume reduction. Our data do, however, point to a significant role of TMEM16A for HlyA-induced volume regulation and lysis in murine erythrocytes. In further support of these data, we found that niflumic acid potentiated HlyA-induced hemolysis of murine erythrocytes. Because CFTR has been proposed to be implicated in Gd^{3+}-induced hemolysis (31), we tested whether this is also the case for HlyA-induced hemolysis but found no difference in response to HlyA in $CFTR^{-/-}$ and $CFTR^{+/+}$ erythrocytes.

Studies have shown that bacterial toxins such as listeriolysin from *Listeria monocytogenes* and the hemolysin from *Vibrio parahemolyticus* provoke shrinkage of erythrocytes and/or PS exposure (32, 33). In agreement, we found that HlyA triggers significant annexin V binding (which indicates PS exposure) in erythrocytes. The HlyA-induced PS exposure was considerably diminished, when the erythrocyte shrinkage was prevented by inhibition of the Ca^{2+} activated K^+ channel, K_{Ca}3.1. This means that K_{Ca}3.1 channel-activation is likely to precede the increase in PS exposure. This finding is supported by an earlier study that showed reduced ionomycin-induced PS exposure in human erythrocytes exposed to K_{Ca}3.1 antagonists (15). In this context, it should be mentioned that $P2X_7$ receptor activation alone is enough to trigger PS exposure in human erythrocytes (22). Our previous study established that $P2X_7$ receptors are activated by HlyA insertion in the erythrocyte membrane and that $P2X_7$ receptor activation is required for lysis of human erythrocytes induced by this toxin (4). Interestingly, Jorgensen *et al.* (20) observed small surface projections within 5 min of HlyA exposure similar to the membrane blebbing seen after $P2X_7$ receptor activation in lymphocytes (34). These findings could imply a role for P2 receptor signaling in HlyA-induced volume regulation, but this requires further investigation.

The K_{Ca}3.1- and TMEM16A-mediated volume reduction and the associated PS exposure are interesting in the context of erythrocyte recognition by macrophages and elimination from the circulation. Through the clear correlation between PS exposure, cell size, and cell age, it has been shown that macrophages use specific detection of PS exposure to eliminate senescent erythrocytes from the circulation (35, 36). Acute damage to the erythrocytes by Ca^{2+} ionophores, energy depletion, oxidative stress, osmotic shock, and malaria infections provoke shrinkage of erythrocytes and/or PS exposure (16, 32, 33, 37–39). Thus, it seems that both senescent and acutely damaged red blood cells are eliminated through the same pathway, and we speculate that K_{Ca}3.1 and TMEM16A activation allow early recognition and removal of erythrocytes attacked by HlyA. Previous studies have shown that erythrocytes from septic patients show severe signs of volume reduction and crenation (40, 41) and PS exposure (42). Patients that survive fulminate sepsis usually present with some degree of anemia, which is partially a consequence of intravascular hemolysis and partially the result of selective removal of damaged red blood cells (42).

Taken together, the present study implies that the process of hemolysis induced by HlyA from *E. coli* is biphasic. Initially, HlyA triggers extensive cellular shape changes and volume reduction. These changes are the consequence of increments in $[Ca^{2+}]_i$, which result in K_{Ca}3.1 and TMEM16A activation and are accompanied by increased PS exposure. This mechanism might be essential for the recognition and removal of HlyA-inserted erythrocytes from the circulation, thereby avoiding intravascular hemolysis during Gram-negative sepsis.

Acknowledgments—We thank Professor Sucharit Bhakdi and Silvia Weiss (University of Mainz, Mainz, Germany) for purifying and providing E. coli α-hemolysin and Joanna Almaca (University of Regensburg, Regensburg, Germany) for measuring osmotic fragility in TMEM16A erythrocytes. Also we thank Rikke Christensen, Anette Thomsen, and Anne B. Strandsby (Aarhus University, Aarhus, Denmark) for technical assistance. We gratefully acknowledge the generous supply of the $TMEM16A^{-/-}$ mice by Dr. Jason Rock and Dr. Brian Harfe (University of Gainesville, Gainesville, Florida), the $CFTR^{-/-}$ mice by Ursula Seidler (Hannover Medical School, Hannover, Germany), and $AQP1^{-/-}$ mice by Alan Verkman (University of California).

REFERENCES

1. Cavalieri, S. J., Bohach, G. A., and Snyder, I. S. (1984) *Microbiol. Rev.* **48,** 326–343
2. Bhakdi, S., Mackman, N., Nicaud, J. M., and Holland, I. B. (1986) *Infect. Immun.* **52,** 63–69
3. Bhakdi, S., Mackman, N., Menestrina, G., Gray, L., Hugo, F., Seeger, W., and Holland, I. B. (1988) *Eur. J. Epidemiol.* **4,** 135–143
4. Skals, M., Jorgensen, N. R., Leipziger, J., and Praetorius, H. A. (2009) *Proc. Natl. Acad. Sci. U.S.A.* **106,** 4030–4035
5. Jorgensen, S. E., Mulcahy, P. F., Wu, G. K., and Louis, C. F. (1983) *Toxicon* **21,** 717–727
6. Menestrina, G., Pederzolli, C., Dalla Serra, M., Bregante, M., and Gambale, F. (1996) *J. Membr. Biol* **149,** 113–121
7. Hoffman, J. F., and Laris, P. C. (1974) *J. Physiol.* **239,** 519–552
8. Rock, J. R., Futtner, C. R., and Harfe, B. D. (2008) *Dev. Biol.* **321,** 141–149
9. Jay, A. W. (1975) *Biophys. J.* **15,** 205–222
10. McManus, M., Fischbarg, J., Sun, A., Hebert, S., and Strange, K. (1993) *Am. J. Physiol.* **265,** C562–C570
11. Hunter, M. J. (1977) *J. Physiol.* **268,** 35–49
12. Knauf, P. A., Fuhrmann, G. F., Rothstein, S., and Rothstein, A. (1977) *J. Gen. Physiol.* **69,** 363–386
13. Almaça, J., Tian, Y., Aldehni, F., Ousingsawat, J., Kongsuphol, P., Rock, J. R., Harfe, B. D., Schreiber, R., and Kunzelmann, K. (2009) *J. Biol. Chem.* **284,** 28571–28578
14. Bratosin, D., Estaquier, J., Petit, F., Arnoult, D., Quatannens, B., Tissier, J. P., Slomianny, C., Sartiaux, C., Alonso, C., Huart, J. J., Montreuil, J., and Ameisen, J. C. (2001) *Cell Death Differ.* **8,** 1143–1156
15. Lang, P. A., Kaiser, S., Myssina, S., Wieder, T., Lang, F., and Huber, S. M. (2003) *Am. J. Physiol. Cell Physiol.* **285,** C1553–C1560
16. Lang, K. S., Duranton, C., Poehlmann, H., Myssina, S., Bauer, C., Lang, F., Wieder, T., and Huber, S. M. (2003) *Cell Death Differ.* **10,** 249–256
17. Sarkadi, B., Szász, I., and Gárdos, G. (1976) *J. Membr. Biol.* **26,** 357–370
18. Borgers, M., Thone, F. J., Xhonneux, B. J., and De Clerck, F. F. (1983) *J. Histochem. Cytochem.* **31,** 1109–1116
19. Short, E. C., and Kurtz, H. J. (1971) *Infect. Immun.* **3,** 678–687
20. Jorgensen, S. E., Hammer, R. F., and Wu, G. K. (1980) *Infect. Immun.* **27,** 988–994
21. Foller, M., Kasinathan, R. S., Koka, S., Lang, C., Shumilina, E., Birnbaumer, L., Lang, F., and Huber, S. M. (2008) *Cell Physiol. Biochem.* **21,** 183–192
22. Sluyter, R., Shemon, A. N., and Wiley, J. S. (2007) *Biochem. Biophys. Res. Commun.* **355,** 169–173
23. Locovei, S., Bao, L., and Dahl, G. (2006) *Proc. Natl. Acad. Sci. U.S.A.* **103,** 7655–7659
24. White, J. G. (1974) *Am. J. Pathol.* **77,** 507–518
25. Hoffman, J. F., Joiner, W., Nehrke, K., Potapova, O., Foye, K., and Wickrema, A. (2003) *Proc. Natl. Acad. Sci. U.S.A.* **100,** 7366–7371
26. Begenisich, T., Nakamoto, T., Ovitt, C. E., Nehrke, K., Brugnara, C., Alper, S. L., and Melvin, J. E. (2004) *J. Biol. Chem.* **279,** 47681–47687
27. Lew, V. L., Tiffert, T., Etzion, Z., Perdomo, D., Daw, N., Macdonald, L., and Bookchin, R. M. (2005) *Blood* **105,** 361–367
28. Grgic, I., Kaistha, B. P., Paschen, S., Kaistha, A., Busch, C., Si, H., Köhler, K., Elsässer, H. P., Hoyer, J., and Köhler, R. (2009) *Pflugers Arch.* **458,** 291–302
29. Huber, S. M., Foller, M., Koka, S., Boini, K. M., Shumilina, E., Mahmud, H., Ruth, P., Sausbier, M., and Lang, F. (2008) *Acta Physiol.* **192,** 54 (abstr.)
30. Myssina, S., Lang, P. A., Kempe, D. S., Kaiser, S., Huber, S. M., Wieder, T., and Lang, F. (2004) *Cell Physiol. Biochem.* **14,** 241–248
31. Stumpf, A., Wenners-Epping, K., Wälte, M., Lange, T., Koch, H. G., Häberle, J., Dübbers, A., Falk, S., Kiesel, L., Nikova, D., Bruns, R., Bertram, H., Oberleithner, H., and Schillers, H. (2006) *Cell Physiol. Biochem.* **17,** 29–36
32. Föller, M., Shumilina, E., Lam, R., Mohamed, W., Kasinathan, R., Huber, S., Chakraborty, T., and Lang, F. (2007) *Cell Physiol. Biochem.* **20,** 1051–1060
33. Lang, P. A., Kaiser, S., Myssina, S., Birka, C., Weinstock, C., Northoff, H., Wieder, T., Lang, F., and Huber, S. M. (2004) *Cell Microbiol.* **6,** 391–400
34. Taylor, S. R., Gonzalez-Begne, M., Dewhurst, S., Chimini, G., Higgins, C. F., Melvin, J. E., and Elliott, J. I. (2008) *J. Immunol.* **180,** 300–308
35. Connor, J., Bucana, C., Fidler, I. J., and Schroit, A. J. (1989) *Proc. Natl. Acad. Sci. U.S.A.* **86,** 3184–3188
36. Connor, J., Pak, C. C., and Schroit, A. J. (1994) *J. Biol. Chem.* **269,** 2399–2404
37. Bratosin, D., Mazurier, J., Tissier, J. P., Estaquier, J., Huart, J. J., Ameisen, J. C., Aminoff, D., and Montreuil, J. (1998) *Biochimie.* **80,** 173–195
38. Bracci, R., Perrone, S., and Buonocore, G. (2002) *Acta Paediatr. Suppl.* **91,** 130–134
39. Lang, K. S., Roll, B., Myssina, S., Schittenhelm, M., Scheel-Walter, H. G., Kanz, L., Fritz, J., Lang, F., Huber, S. M., and Wieder, T. (2002) *Cell Physiol. Biochem.* **12,** 365–372
40. Piagnerelli, M., Zouaoui Boudjeltia, K., Brohee, D., Vereerstraeten, A., Piro, P., Vincent, J. L., and Vanhaeverbeek, M. (2007) *J Clin. Pathol.* **60,** 549–554
41. Piagnerelli, M., Boudjeltia, K. Z., Gulbis, B., Vanhaeverbeek, M., and Vincent, J. L. (2007) *Trans. Alt. Transf. Med.* **9,** 143–149
42. Kempe, D. S., Akel, A., Lang, P. A., Hermle, T., Biswas, R., Muresanu, J., Friedrich, B., Dreischer, P., Wolz, C., Schumacher, U., Peschel, A., Gotz, F., Doring, G., Wieder, T., Gulbins, E., and Lang, F. (2007) *J. Mol. Med.* **85,** 273–281